

Adaptive Optics Sky Coverage for Dome C Telescopes

J. S. LAWRENCE, M. C. B. ASHLEY, AND J. W. V. STOREY

School of Physics, University of New South Wales, Sydney, NSW 2052, Australia; jl@phys.unsw.edu.au

L. JOLISSAINT

Observatory of Leiden, Leiden 2333, The Netherlands

AND

T. TRAVOUILLO

California Institute of Technology, Pasadena, CA

Received 2008 June 18; accepted 2008 September 03; published 2008 September 30

ABSTRACT. The unique atmospheric characteristics found at Dome C on the Antarctic plateau offer significant advantages for the operation of adaptive optics systems. An analysis is presented here comparing the performance of adaptive optics systems on telescopes located at Dome C with similar systems located at a mid-latitude site. The large coherence length, wide isoplanatic angle, and long coherence time of the Dome C atmosphere allow an adaptive optics system located there to correct to high order, observe over wide fields and use faint guide stars, resulting in a lower total wavefront error and a significant increase in sky coverage factor than can be achieved at a typical mid-latitude site. While the same performance could in principle be achievable at mid-latitude sites, this would only occur under exceptionally stable atmospheric conditions that are likely to occur on only a few nights per year.

1. INTRODUCTION

The Earth's turbulent atmosphere limits the spatial resolving power of ground-based telescopes. Current and proposed large telescopes, with apertures from 8–42 m, thus require highly effective adaptive optics (AO) systems, which correct atmospheric turbulence-induced phase distortions of the optical wavefront. A limitation to the degree of correction achievable with an AO system arises from errors that depend strongly on the atmospheric characteristics of the telescope site; specifically Fried's parameter, r_0 , the isoplanatic angle, θ_0 , and the atmospheric time constant, τ_0 . These parameters define (respectively) the length, angle, and time over which the atmospheric phase distortions are coherent.

The French/Italian Dome C station (Candidi & Lori 2003) on the Antarctic plateau is located at an altitude of 3250 m above sea level. Site testing data from the last few winter seasons (Lawrence et al. 2004a; Agabi et al. 2006; Trinquet et al. 2008) have confirmed earlier expectations (Gillingham 1991; Marks 2002) that the atmosphere above Dome C is exceptionally calm and stable. Above a strongly turbulent near-surface layer of height approximately 35 m, each of the atmospheric parameters relevant for AO systems, r_0 , θ_0 , τ_0 , is a factor 2–3 better (larger, wider, longer) than typically found at the best mid-latitude sites. An AO system on a Dome C telescope should thus provide a much more effective correction of atmospheric turbulence (see e.g., Lawrence 2004a). This paper quantifies the performance of Dome C AO systems relative to mid-latitude site

AO systems in terms of the achievable sky coverage factor, using the PAOLA (Jolissaint et al. 2006) analytical AO simulation code. Both Natural Guide Star (NGS) and Laser Guide Star (LGS) systems are considered for telescope diameters of 8, 20, and 30 m.

For this analysis it is assumed that the Dome C telescope is placed on a tower that is high enough to put it above the strong boundary layer turbulence. This is not expected to represent a significant technological difficulty as many existing large telescopes are at similar heights above ground level (e.g., the Anglo-Australian Telescope [AAT] at 26 m, the Canada-France-Hawaii Telescope [CFHT] at 28 m, the European Southern Observatory [ESO] 3.6 m at 30 m, and the 4 m Nicholas U. Mayall Telescope at 57 m). A very stiff 30-m-high open tower has been proposed for the Pathfinder for a Large Optical Telescope [PILOT] Dome C telescope (Saunders et al. 2008) based on the design of Hammerschlag et al. (2006), similar to that used for the 15 m high Dutch Open Telescope tower on La Palma.

There are many other advantages of Dome C as an astronomical observatory site. The extremely low atmospheric temperatures result in a significant reduction in the atmospheric thermal emission (Walden et al. 2005; Lawrence 2004b). Weak atmospheric scintillation leads to gains in photometric precision and narrow-angle astrometric precision (Kenyon et al. 2006). Results to date suggest an exceptionally high fraction of cloud-free conditions (Ashley et al. 2005a; Mosser & Aristidi

2007). Very low surface wind speeds (Aristidi et al. 2005a) reduce structural requirements on telescope mounts and domes. Such factors must ultimately be weighed against the disadvantages of the Antarctic location, such as the reduced accessibility, reduced total astronomical dark-time (Kenyon & Storey 2006), the potential for ice formation on optical surfaces (Durand et al. 2007), and any engineering constraints arising from the extremely cold temperatures (Ashley et al. 2004; Strassmeier et al. 2007).

2. MODELS

2.1. Turbulence Models

Atmospheric turbulence at Dome C has been measured by a number of different methods. Summertime meteorological balloon measurements and Automatic Weather Station data show very low wind speeds at ground level, a lack of strong winds at high altitudes, and thermal profiles indicative of weak turbulence (Aristidi et al. 2005a). Differential Image Motion Monitor (DIMM) data obtained over several summer seasons (2002–2005) demonstrated that Dome C was a very good daytime observatory with a median seeing (above 8.5 m) of $0.55''$ (Aristidi et al. 2005b). A strong diurnal variation was also observed that included periods of exceptional seeing (down to $0.14''$) in the local afternoon (when the surface layer is isothermal).

The first wintertime turbulence measurements were based on a combination of sonic RADAR (SODAR) and Multi-Aperture Scintillation Sensor (MASS) instruments (Travouillon et al. 2002; Kornilov et al. 2003; Lawrence et al. 2004b). These instruments, which were sensitive to turbulence above ~ 30 m, obtained data over a six week period (March–May) in 2004, and demonstrated an exceptionally low integrated seeing ($0.27''$) above this layer (Lawrence et al. 2004a). In 2005 several ground-level DIMMs were operated, and a series of microthermal balloons were launched throughout the winter. Two data sets from the microthermals have been published (Agabi et al. 2006; Trinquet et al. 2008). These data showed that while the ground-level seeing was relatively poor ($1.4''$ median at 8.5 m), the majority of turbulence was confined to within ~ 35 m of the surface. Above this layer, the seeing, isoplanatic angle, and atmospheric coherence time were in agreement (within statistical error ranges) with the MASS/SODAR results from the previous season.

Figure 1 shows the cumulative distribution of seeing, isoplanatic angle, and coherence time for Cerro Paranal taken over the period 1999–2005.¹ While the DIMM seeing measurements are statistically significant, a strong trend toward worse seeing is evident over the period examined. The Paranal isoplanatic angle estimates rely on scintillation measurements with an accuracy

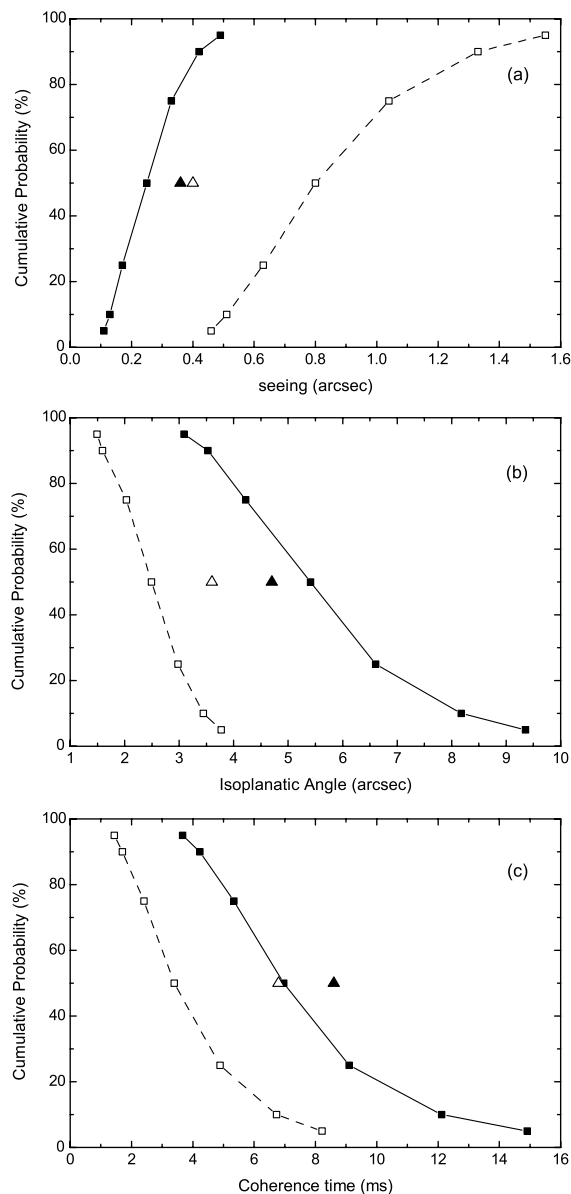


FIG. 1.—Cumulative distribution for (a) seeing, (b) isoplanatic angle, and (c) coherence time for the model atmospheres. Solid-squares represent MASS/SODAR Dome C data (sensitive above 30 m). Open squares are from Cerro Paranal DIMM/balloon data. Triangles show the median values from Dome C microthermal balloons integrated from 30 m (solid triangles from Agabi et al. 2006, open-triangles from Trinquet et al. 2008). All parameters refer to zenith observation at 500 nm.

of 10%, and the Paranal coherence time estimates rely on a limited number of balloon soundings giving an accuracy of 20% (see Sarazin & Tokovinin 2002). Also shown in Figure 1 are the cumulative distributions from the MASS/SODAR 2004 Dome C data set (Lawrence et al. 2004a), and the median values reported from 2005 wintertime microthermal balloon launches at Dome C from both Agabi et al. (2006) and Trinquet et al. (2008).

¹ See the European Southern Observatory Web site Astroclimatology of Paranal at <http://www.eso.org/gen-fac/pubs/astclim/paranal/seeing/adaptive-optics/>.

A seven-layer model of the atmospheric turbulence and wind-speed distribution is employed here for the AO simulations. The refractive index structure constant, C_N^2 , profiles from Cerro Paranal are based on a small number of published microthermal balloon flights (Le Louarn et al. 2000). The profiles from Dome C are based on the MASS/SODAR data². The Cerro Paranal C_N^2 profiles are scaled, and the MASS/SODAR C_N^2 profiles are selected, to match the 10%, 25%, 50%, 75%, and 90% best values for r_0 and θ_0 at each site. For both sites the wind speed profiles are modeled as a Gaussian distribution scaled to give an appropriate value (i.e., 10%, 25%, 50%, 75%, and 90% conditions) for the atmospheric coherence time.

A 30 m outer scale, L_0 , is assumed for all sites. Recent results indicate that the atmospheric outer scale at Dome C may be as small as 10 m (Ziad et al. 2008). The performance metrics for Dome C should thus be considered conservative, as for large-aperture telescopes a small value of L_0 acts to reduce the power in the lowest-order aberration modes.

2.2. Metrics and AO System Parameters

The development of Dome C as an astronomical observatory is now commencing with the deployment of the 80-cm International Robotic Antarctic Infrared Telescope (IRAIT) mid-infrared telescope (Tosti et al. 2006). The next step will likely consist of a 2.4-m class telescope, such as PILOT (Burton et al. 2005; Saunders et al. 2008). Later generation facilities will need to be much larger to take full advantage of the atmospheric conditions. To ascertain the full potential of the site, the AO system performance of 8-, 20-, and 30-m telescopes (each with a filled aperture primary mirror with a 12.5% secondary obscuration) is modeled here. There are already several proposals for facilities of this scale at Dome C, e.g., the 8.4 m Large Antarctic Plateau Clear-Aperture Telescope (LAPCAT; Storey et al. 2006), and the Antarctic Giant Magellan Telescope (Angel et al. 2004).

The performance of an AO system can be quantified by many parameters. Here the Strehl ratio, representing the ratio of the on-axis corrected point-spread function (PSF) intensity to the diffraction-limited on-axis intensity, and the 50% encircled energy diameter, representing the angular diameter enclosing half of the total intensity, are used. A science wavelength of 1.65 μm (i.e., H band) is considered for the majority of simulations. The Strehl ratio (and encircled energy) achievable with a given AO system will vary depending on the magnitude and separation angle of the guide star used. These parameters can be combined by using the sky coverage factor as a metric. This represents the probability of finding an appropriate magnitude star within a field size which minimizes all errors and produces the highest Strehl ratio (see, e.g., Olivier & Gavel 1994). The star density

for a Galactic latitude of 50° derived from the model of Bachall & Soneira (1980) is used here.

An important design choice for any AO system is the wavefront-sensor subaperture pitch. Typical AO systems employ a series of wavefront-sensor geometries with a size matched to provide the best performance at a range of guide star magnitudes. For simplicity, and for a valid comparison between the sites, a fixed subaperture pitch is used for all guide star magnitudes, sites, and telescope sizes. This is set to 0.5 m (projected on the primary mirror plane), and is matched to the actuator spacing of the deformable mirror. This is consistent with the largest Shack-Hartmann arrays currently employed on 8–10 class telescopes. For 8-, 20-, and 30-m telescopes this corresponds to 16×16 , 40×40 , and 60×60 arrays with 200, 1240, and 2800 total number of actuators, respectively.

Other parameters adopted for the AO system simulation are a wavefront-sensor read noise of 5 electrons, a fixed delay time of 1 ms (consistent with current and proposed facilities), and a guide star temperature of 6000 K (corresponding to a G type star). The wavefront sensor has a ~ 400 nm bandwidth centred at 600 nm, with a maximum total efficiency of 30% (arising from losses due to CCD quantum efficiency, and optical and atmospheric transmission). For each guide star magnitude, the wavefront-sensor integration time is optimized to give the highest Strehl, as fainter stars require longer integration times. For the LGS simulation a 92 km sodium layer laser guide star with a projected diameter of 4" is used, with a wavefront-sensor noise-equivalent-angle of 0.05". For both NGS and LGS simulations static wavefront errors resulting from high frequency primary mirror and instrument aberrations are ignored. For real systems this “nonfitting” error can be significant, typically in the range 150–300 nm rms, depending on the quality of optical surfaces and the wavefront-sensor subaperture pitch (Racine 2006). All performance metrics used here assume observations at zenith.

2.3. Adaptive Optics Simulation Code

The analytic code PAOLA is used here to model the AO-corrected PSF (Jolissaint et al. 2006). Such a code differs from end-to-end Monte-Carlo (MC) based AO modeling codes because the long exposure PSF is directly obtained, while MC codes produce instantaneous AO-corrected PSF that need to be averaged. Comparisons between PAOLA and other MC codes have shown that the gain in modeling time is a factor of ~ 100 , thus it is possible to explore the AO parameter space in detail. It is important to note that if analytical tools are well adapted to the comparison of sites as done here, absolute numbers should be considered with caution; particularly in the LGS case, where more simplifying assumptions have been used than in the NGS case. MC codes are therefore essential when designing a given AO system, where it is important to take into account second order, nonlinear effects that cannot be modeled easily with analytical codes.

²See the archive of Dome C AASTINO data at http://www.phys.unsw.edu.au/~jl/aastino_data/.

PAOLA uses the relationship between the AO-corrected phase spatial power spectrum (PSD) and the long exposure AO optical transfer function (OTF; Jolissaint et al. 2006). For LGS modeling, we use the Sasiela (1994) description of focal anisoplanatism PSD (cone effect), and include its correlation with angular anisoplanatism. As tip-tilt cannot be corrected by an LGS-based AO system, the tip-tilt part of the phase turbulent spectrum is filtered out before applying the LGS AO spatial filter model to get the residual LGS residual phase PSD. The tip-tilt part, on the other hand, is filtered by an NGS-based AO filter, and added to the LGS residual PSD. While this approach permits the calculation of the phase variance associated to the focal/angular anisoplanatism, its validity to compute the associated OTF (as we do for NGS-based modeling) has not been proven strictly, yet: comparison with the PSF calculated from Monte-Carlo codes in LGS mode still needs to be done. Any errors introduced here would have a direct impact on the structure of the PSF wings. This said, in our study, PSFs are only used to compute integrated energy metrics, where the fine details of the PSF wings are somewhat integrated out. Therefore, we are relatively confident in the validity of our model prediction, at least in the first-order approach used here. It is important to note that NGS modeling does not suffer from these uncertainties: Monte-Carlo-based cross checks have been done several times, always showing excellent agreement with the analytical approach prediction of the PSF structure (Jolissaint et al. 2006; Neichel et al. 2008). The following components of the phase PSD are modeled in PAOLA: uncorrected high spatial frequency phase (above the deformable mirror cutoff frequency), Shack-Hartmann wavefront-sensor spatial aliasing, anisoplanatism, AO loop servo-lag, and wavefront-sensor noise. In LGS mode, we also include cone anisoplanatism and tip-tilt correction error.

3. RESULTS

3.1. Error Sources

The relative contribution of the main NGS error sources for the Dome C and Cerro Paranal median atmospheres is illustrated in Figure 2, which demonstrates the effects of (a) wavefront-sensor-noise and bandwidth errors for an on-axis guide star of varying magnitude; and (b) anisoplanatic error for a bright guide star as a function of separation angle. The longer coherence length of the Dome C atmosphere results in an improved fitting of the perturbed wavefront by the deformable mirror, giving higher Strehl for brighter stars or smaller separations. The longer coherence time of the Dome C atmosphere allows a longer integration time (where this integration time is optimized for each guide star brightness); guide stars ~ 2 magnitudes fainter can thus be used. The wider isoplanatic angle of the Dome C atmosphere allows guide stars at larger angular separations resulting in ~ 2 – 4 times wider fields of correction.

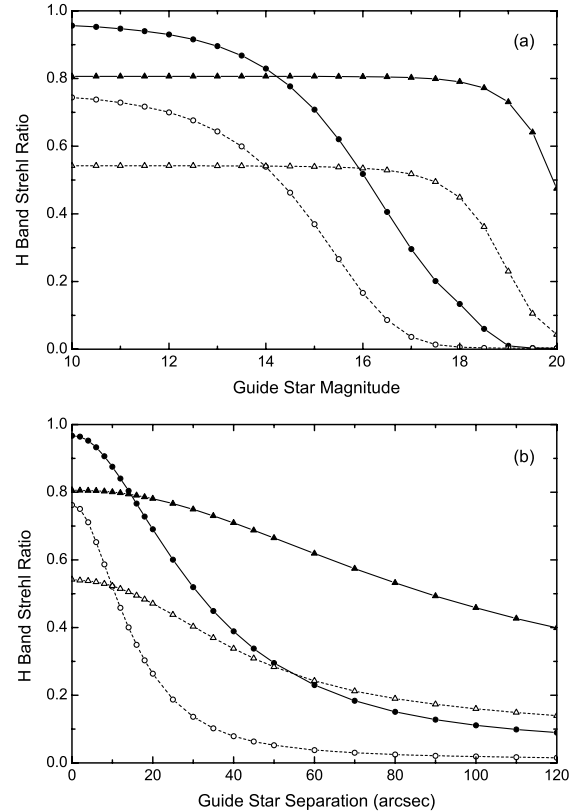


FIG. 2.—(a) H -band Strehl ratio vs. on-axis guide star magnitude; (b) H -band Strehl ratio vs. separation angle for a bright guide star. Each plot shows results for Dome C (solid lines) and Cerro Paranal (dashed lines) median atmospheres for NGS (circles) and LGS (triangles) systems on an 8-m telescope. All metric here, and in the following figures, refer to observations at zenith.

For an LGS system the error sources arise primarily from tip-tilt measurement and correction, as this must be accomplished with a natural guide star. Compared to high-order correction, fainter stars can be used for tilt correction, as the wavefront sensing aperture is much larger. Additionally, the atmospheric tilt isoplanatic (or isokinetic) angle is significantly larger than the (high-order) isoplanatic angle, allowing wider guide star separation angles. These factors allow an LGS system to operate with fainter stars over wider fields than an NGS system, as illustrated in Figure 2. Similar to the NGS case, a Dome C LGS tip-tilt system can achieve higher Strehl over wider fields with fainter stars than a mid-latitude system.

An additional error source, cone anisoplanatism, is introduced for an LGS system. This arises (for a sodium-layer LGS) from the unsensed turbulence at the edge of the aperture. This error depends on wavelength and telescope diameter, and on the vertical distribution of turbulence. The Strehl ratio resulting from this error source alone is illustrated in Figure 3 for Dome C and Cerro Paranal atmospheres with 8- and 20-m telescopes. At a typical mid-latitude site this error restricts single LGS systems to wavelengths longward of H band for high

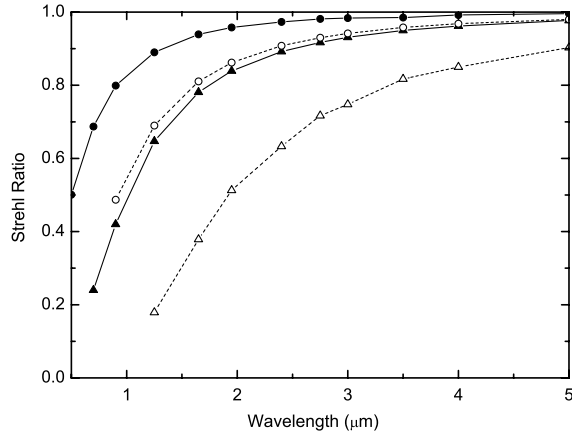


FIG. 3.—Strehl ratio resulting from cone anisoplanatism as a function of wavelength for a single sodium LGS at an altitude of 92 km on 8-m (circles) and 20-m (triangles) telescopes, with Dome C (solid lines) and Cerro Paranal (dashed lines) atmospheres.

Strehl correction on an 8-m telescope and significantly reduces the obtainable Strehl for near-infrared observations on an extremely large telescope (ELT). This necessitates the use of multiple guide stars for mid-latitude ELTs, i.e., the Laser Tomography AO configuration. At Dome C this error allows reasonable near-infrared correction with a single LGS, even on a 20 m telescope.

3.2. Natural Guide Star AO

The results of the NGS AO simulation for Dome C and Cerro Paranal median atmospheres are shown in Figure 4, which gives H -band Strehl and encircled energy versus sky coverage factor for 8-, 20-, and 30-m telescopes. This figure illustrates the limitations of NGS AO systems at typical mid-latitude locations; reasonable correction (Strehl >0.2) at H band can only be achieved over a small fraction ($\sim 1\%$) of the sky. The combined advantages of the Dome C atmosphere illustrated in Figure 2 significantly increase (by a factor of 20–100) the available sky coverage on any size telescope. On an 8-m Dome C telescope, for example, a large fraction of the sky at this relatively high Galactic latitude can be corrected at this wavelength.

The relevance of these NGS AO system comparisons can be questioned, however, as the majority of large-scale mid-latitude observatories either currently employ or intend to employ LGS AO systems. This is addressed in the next section.

3.3. Laser Guide Star AO

Results from the LGS AO system simulation are shown in Figure 5. At both sites the performance of the LGS system is constant over a large fraction of the sky, falling off at sky coverage factors greater than 10%–30%, where limitations arise from the tip-tilt correction system. For low sky coverage factors, where tip-tilt errors are negligible, the limitations primarily arise

from a combination of cone anisoplanatic error and LGS system wavefront-sensor noise. These errors are both lower for the Antarctic atmosphere, leading to higher Strehl ratios, e.g., for an 8-m telescope a maximum Strehl of 0.80 is found at Dome C compared to 0.55 for Cerro Paranal.

The corrected resolution (encircled energy) depends on the Strehl ratio, the telescope size, and the uncorrected atmospheric seeing. The exceptional natural seeing at Dome C, and the high corrected Strehl ratio results in an encircled energy diameter for the 8-m Dome C telescope, which is smaller than that obtainable with either 8-, 20-, or 30-m Cerro Paranal telescopes, for all sky coverage factors. This illustrates the importance of cone anisoplanatism, which increases for increasing telescope size. As discussed in § 3.1, ELT class (20 m and above) telescopes at mid-latitude sites require multiple laser guide stars to mitigate against this. It is shown here, however, that reasonable performance over a large fraction of the sky is achievable with a single laser guide star on an Antarctic ELT class telescope.

Given the relative complexities of setting up and maintaining an LGS AO system in the harsh Dome C environment with a limited number of support staff available, a more valid performance comparison is between the Dome C NGS system and the mid-latitude LGS system. Comparing Figure 4 to Figure 5, the Dome C NGS system achieves comparable performance to that of the Cerro Paranal LGS system for relatively large sky coverage factors (greater than $\sim 10\%$). The real advantage of the Dome C system, however, is that for low sky coverage factors, i.e., low probability fields ($<0.5\%$) with relatively bright ($m_v > 15$) stars, diffraction-limited observations are possible with a single NGS AO system for telescopes of up to 30 m diameter.

3.4. Turbulence Variability

The characteristics of the atmospheric turbulence at any site can vary significantly over time. The sky coverage factor of an AO system for the median turbulence conditions (as examined in the previous sections) represents the expected minimum level of performance achievable for half of the observing time. A more thorough site-to-site comparison is obtained by examining the performance for a range of atmospheric conditions. Figure 6 shows the H -band Strehl ratio versus sky coverage factor for the 10%, 25%, 50%, 75%, and 90% best atmospheric models for Dome C and Cerro Paranal.

For both sites, the difference between the 10% best and the 10% worst atmospheric conditions represents a factor of 50–100 in sky coverage. The worst 10% conditions at Dome C are equivalent to the 10% best conditions at Cerro Paranal. We thus expect that the mid-latitude site may obtain conditions similar to the Dome C median for a few percent of the time, i.e., a few nights per year. The best conditions at Dome C, however, provide exceptional performance, with resolution approaching the diffraction limit across the majority of the sky, that is not likely to arise elsewhere.

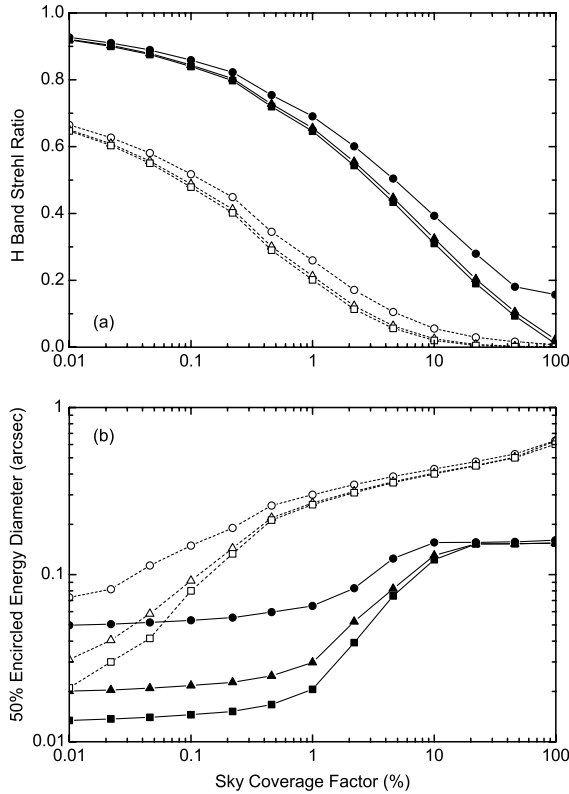


FIG. 4.—*H*-band (a) Strehl ratio and (b) 50% encircled energy diameter as a function of sky-coverage factor for a single deformable mirror NGS AO system with Dome C (solid lines) and Cerro Paranal (dashed lines) median atmospheres. Telescopes of diameter 8 m (circles), 20 m (triangles), and 30 m (squares) are shown.

It should be noted that this is meant as an illustrative rather than a statistically robust analysis of the turbulence variability. The derivation of the percentile-ranked atmospheric models for each site assumes that the variables r_0 , θ_0 , and τ_0 are statistically dependent. In general, low values of total integrated seeing occur when the isoplanatic angle and coherence time are respectively, large and long; however, this is not always the case. The effect of realistically modeling this situation, e.g., by running the simulation code for hundreds of independent profiles for each site, would be to reduce the spread of performance about the median value for each site, compared with what has been modeled here.

3.5. Science Wavelength

AO system performance is a strong function of wavelength, as a higher level of phase correction is required for shorter wavelengths. The previous simulations have considered observations at *H*-band ($1.65 \mu\text{m}$). This waveband, along with other near-infrared windows at *J*-band ($1.25 \mu\text{m}$), and *K*-band ($2.2 \mu\text{m}$) is where the majority of classical AO systems in

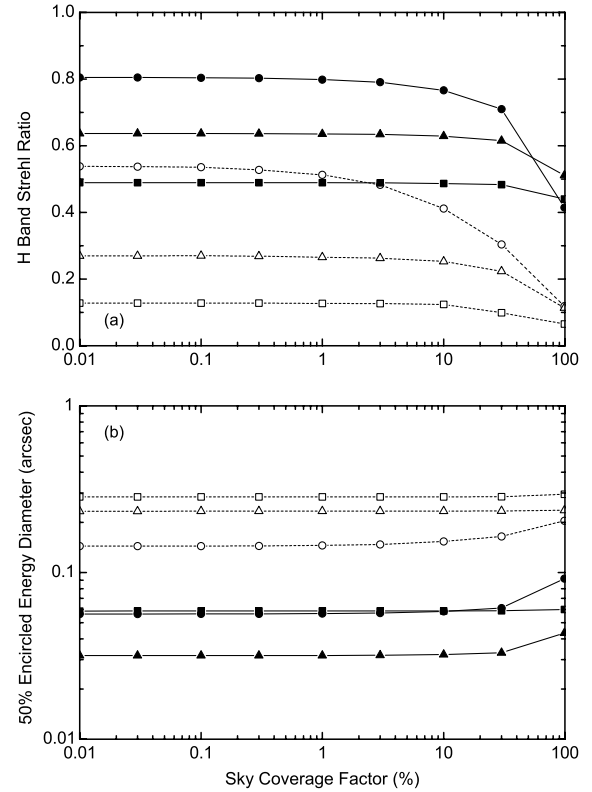


FIG. 5.—*H*-band (a) Strehl ratio and (b) 50% encircled energy diameter as a function of sky-coverage factor for a single deformable mirror LGS AO system with Dome C (solid lines) and Cerro Paranal (dashed lines) median atmospheres. Telescopes of diameter 8 m (circles), 20 m (triangles), and 30 m (squares) are shown.

use today operate. Improving the atmospheric site conditions has the effect of reducing the system absolute wavefront error. This results in either a higher Strehl ratio at a given wavelength, as shown previously, or the same Strehl ratio at a shorter wavelength.

The relative performance of the two sites in wavelength parameter space is investigated in Figure 7, for both NGS and LGS systems on an 8-m telescope. A sky coverage factor of 10% is considered in all cases. At this sky coverage factor, the Dome C NGS Strehl ratio is similar to the Cerro-Paranal LGS Strehl ratio for *all* wavelengths. For wavelengths less than $\sim 1.6 \mu\text{m}$, where partial correction is achieved at both sites, although the Strehl ratio is the same, the 50% encircled energy diameter achieved at Dome C is significantly smaller than at Cerro Paranal. This smaller encircled energy diameter arises from the superior free-atmosphere seeing at Dome C. For the Dome C LGS system, a unique parameter space is enabled. Reasonable levels of correction are obtainable for wavelengths as low as $0.5 \mu\text{m}$. For lower probability fields this Dome C advantage is even greater, with correction possible at wavelengths approaching the visible even with an NGS system.

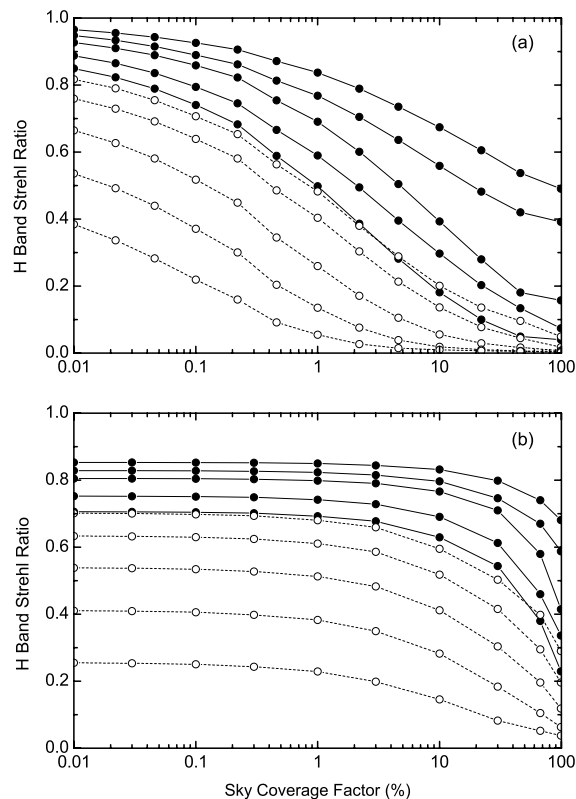


FIG. 6.—*H*-band Strehl ratio as a function of sky-coverage factor for a single deformable mirror (a) NGS and (b) LGS AO system on an 8-m telescope at Dome C (solid lines, solid circles) and Cerro Paranal (dashed lines, open circles). For both sites, atmospheric models corresponding to the 10%, 25%, 50%, 75%, and 90% best conditions are shown (top to bottom curves, respectively).

3.6. Dome C Ground Layer

Both the current data sets on the Dome C turbulence distribution suffer some disadvantages. The MASS/SODAR results have very good temporal coverage but only for a 6 week period at the beginning of winter. It is likely that this introduces some selection effect as the turbulence conditions may change throughout the year. Additionally, the atmospheric coherence time derived from MASS is known to be an underestimate of the actual value (Travouillon et al. 2008, in preparation), although this may be somewhat compensated by unsensed turbulence and wind speed in the lower surface layer. In addition, the boundary layer height is not well defined by the first data point from the SODAR. The microthermal balloon results offer a much higher spatial sampling of the free atmospheric turbulence and the boundary layer, and sample the atmosphere at a range of times throughout the year. However, they do not provide information on short-term variability and data from only a small number of profiles has been published. Using a model derived from the Agabi et al. (2006) results, both the microthermal and MASS/SODAR data sets predict very similar performance. As shown in Figure 8, the difference is ~ 0.05 in

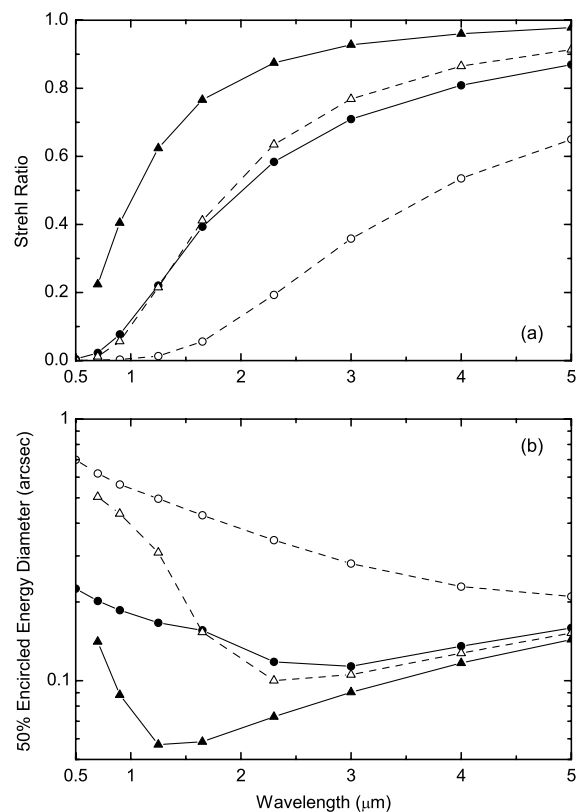


FIG. 7.—(a) Strehl ratio and (b) 50% encircled energy diameter vs. wavelength for an 8-m telescope at 10% sky-coverage factor with Dome C (solid line, solid symbols) and Cerro Paranal (dashed line, open symbols) median atmospheres. Both NGS (circles) and LGS (triangles) systems are shown.

Strehl ratio for a given sky coverage factor, or a factor 1.5–2 in sky coverage for a given Strehl. This small difference arises because the balloon measurements report a smaller value of r_0 but a higher coherence time. The isoplanatic angle derived from both instruments is similar. The performance predicted using a model derived from Trinquet et al. (2008) is degraded relative to the MASS/SODAR model, particularly for high sky coverage factors; the difference is ~ 0.1 in Strehl ratio for a given sky coverage factor, or a factor of 4–6 in sky coverage for a given Strehl. This difference is primarily a result of the low isoplanatic angle derived by the full microthermal data set. This median value is, however, based on only a few balloons that reach the highest altitudes in midwinter. Recent generalized seeing monitor (GSM) results from Dome C (Ziad et al. 2008) show an isoplanatic angle that is larger than measured with the microthermals, although the GSM data are predominantly obtained from the summer and autumn periods.

No data currently exist on the temporal variability of the vertical distribution of the Dome C turbulent boundary layer, although several instruments have been proposed to measure this (Bonner et al. 2008). It is likely that some fraction of the turbulence within the boundary layer will reach the height

of the telescope for some fraction of the time. Additionally, for a tower-mounted telescope there may be some turbulence generated by the tower, the telescope structure, or the telescope enclosure. To model these effects an extra turbulent layer is added at 30 m that represents some fraction of the ground-layer turbulence (i.e., the layer that gives 1.4" average at ground level measured by the DIMMs). This is illustrated in Figure 8. For a layer that represents 20% of the ground-level turbulence, there is a reduction in the Strehl value of ~ 1.0 , compared to the MASS/SODAR median model. Similar to the Trinquet et al. (2008) model, this has little effect at low sky coverage factors but begins to degrade the achievable encircled energy at high sky-coverage factors.

For comparison, Figure 8 also shows the achievable resolution for operation of an 8-m telescope at Dome C ground level. In this case the performance is comparable with a mid-latitude site for large sky-coverage factors, but significantly worse for low probability fields. This illustrates, as may have been expected, that for classical AO there is a necessary requirement that the telescope is placed above the turbulent boundary layer

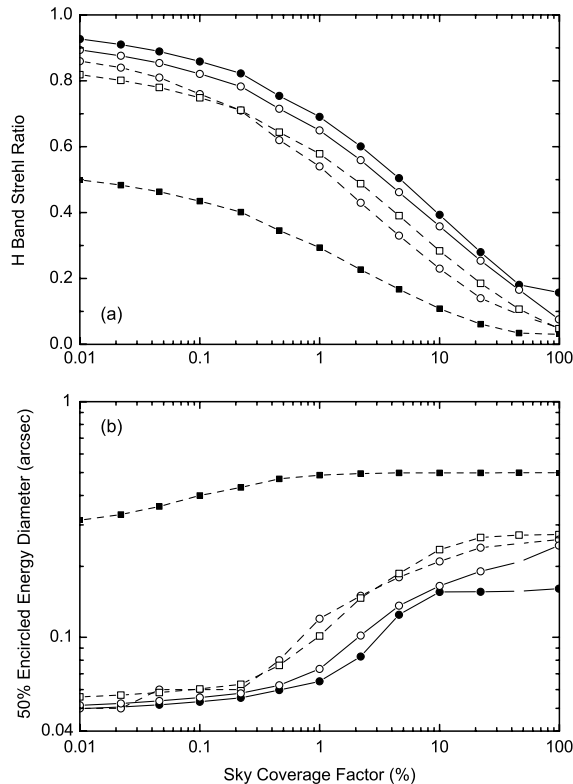


FIG. 8.—*H*-band (a) Strehl ratio and (b) 50% encircled energy diameter vs. sky-coverage factor for the Dome C median atmosphere model from MASS/SODAR data (solid line, solid circles) compared to the Dome C microthermal balloon models (solid line, open circle from Agabi et al. 2006 and dashed line, open circle from Trinquet et al. 2008). Also shown is Dome C performance at ground level (dashed line, solid squares) and on a tower with 20% of ground-layer turbulence added at the telescope height (dashed line, open squares).

in order to take full advantage of the Dome C site conditions. It is likely that performance, relative to this, could be significantly improved with a Ground-Layer AO system at Dome C, specifically designed for the unique turbulent profile. This is addressed by Travouillon et al. (2008, in preparation).

4. CONCLUSIONS

There are many advantages and disadvantages of Dome C, on the Antarctic plateau, as an astronomical observatory site. To fully realize the potential of the location and to be competitive with current well-established and future planned mid-latitude and space facilities, large diameter (8 m and above) telescopes will be required. It is important to understand the potential of such large-scale facilities now, at the time when smaller-scale pilot facilities are being designed and deployed. Here we have concentrated on quantifying the benefits of the Dome C atmospheric conditions for large-telescope AO systems.

More data over several seasons are needed to ascertain the height and distribution of the turbulent boundary layer at Dome C, as it is important to understand the exact requirements for a structure to elevate a telescope above this layer. Additionally, more data on the temporal evolution of the distribution and strength of high-altitude turbulence are required to give a statistically meaningful appraisal of the site. The results presented here, however, have demonstrated the significant potential for operating classical adaptive optics systems on large Dome C telescopes. The excellent atmospheric seeing reduces errors in atmospheric fitting, the high atmospheric coherence time allows the use of fainter guide stars, and the large isoplanatic angle results in a wider field of correction. These factors result in an increase in the sky coverage achievable for a Dome C AO system compared to a typical mid-latitude AO system.

Any large-scale Antarctic plateau astronomical facility will be required to be as simple and robust as possible, probably precluding (at least in the early stages) the deployment of complex high-power laser systems, or multi-conjugate optical systems. Such systems are currently operational now at a number of mid-latitude sites. An Antarctic telescope must therefore compete with such facilities. It has been shown here that a Dome C NGS AO system should perform as well as a mid-latitude LGS system for high sky-coverage factor observations (i.e., for high-probability fields). It can be argued that this is not in itself enough motivation for the development of such a facility (i.e., it can be done just as well at a current observatory), but that any proposed Antarctic telescope should open up a new parameter space not accessible elsewhere. As shown here, one of the real niches for an Antarctic AO system, where this is true, is in the observation of low-probability, highly targeted fields (i.e., those with relatively bright guide stars available), under the best Dome C atmospheric conditions (conditions that are not likely to ever occur elsewhere). Under such conditions observations are possible at higher resolution and shorter wavelengths than achievable at any other ground-based site.

We thank Andrei Tokovinin from Cerro Tololo Inter-American Observatory for helpful input into developing the AO system model parameter space used for site-to-site comparison, and for comments on the manuscript. We thank the Australian Research Council for its support through the Discovery Projects

and Linkage International schemes, and the EU for its support via the ARENA Coordination Action. We also thank our colleagues in Europe, the US, and Australia for helpful and stimulating discussions, and colleagues from the polar agencies AAD, IPEV, and PNRA for ongoing support and encouragement.

REFERENCES

- Agabi, A., Aristidi, E., Azouit, M., Fossat, E., Martin, F., Sadibekova, T., Vernin, J., & Ziad, A. 2006, *PASP*, 118, 344
- Angel, J. R. P., Lawrence, J. S., & Storey, J. W. V. 2004, *Proc. SPIE*, 5382, 75
- Aristidi, E., et al. 2005a, *A&A*, 430, 739
- . 2005b, *A&A*, 444, 651
- Ashley, M. C. B., Burton, M. G., Calisse, P. G., Phillips, A., & Storey, J. W. V. 2005a, in *Highlights of Astronomy*, Vol. 13, ed. O. Engvold (San Francisco: ASP), 936
- Ashley, M. C. B., Burton, M. G., Lawrence, J. S., & Storey, J. W. V. 2004, *Astron. Nach.*, 325, 619
- Bahcall, J. N., & Soneira, R. M. 1980, *APJS*, 44, 73
- Bonner, C. S., Ashley, M. C. B., Lawrence, J. S., Storey, J. W. V., Luong-Van, D. M., & Bradley, S. G. 2008, *Proc. SPIE*, 7014, 70146I
- Burton, M. G., et al. 2005, *Publ. Astron. Soc. Australia*, 22, 199
- Candidi, M., & Lori, A. 2003, *Mem. Soc. Astron. Italiana*, 74, 29
- Durand, G., et al. 2007, *EAS Pub. Ser.*, 25, 77
- Gillingham, P. R. 1991, *Proc. Astron. Soc. Australia*, 9, 55
- Hammerschlag, R. H., Bettonvil, F. C. M., & Jägers, A. P. L. 2006, *Proc. SPIE*, 6273, 62731O
- Jolissaint, L., Veran, J. P., & Conan, R. 2006, *J. Opt. Soc. Am. A*, 23, 382
- Kenyon, S. L., Lawrence, J. S., Ashley, M. C. B., Storey, J. W. V., Tokovinin, A., & Fossat, E. 2006, *PASP*, 118, 924
- Kenyon, S. L., & Storey, J. W. V. 2006, *PASP*, 118, 489
- Kornilov, V., et al. 2003, *Proc. SPIE*, 4839, 837
- Lawrence, J. S. 2004a, *AO*, 43, 1435
- . 2004b, *PASP*, 116, 482
- Lawrence, J. S., Ashley, M. C. B., Kenyon, S., Storey, J. W. V., Tokovinin, A., Lloyd, J. P., & Swain, M. 2004b, *Proc. SPIE*, 5489, 174
- Lawrence, J. S., Ashley, M. C. B., Travouillon, T., & Tokovinin, A. 2004a, *Nature*, 431, 278
- Le Louarn, M., Hubin, N., Sarazin, M., & Tokovinin, A. 2000, *MNRAS*, 317, 535
- Marks, R. 2002, *A&A*, 385, 328
- Mosser, B., & Aristidi, E. 2007, *PASP*, 119, 127
- Neichel, B., Fusco, T., Conan, J., Petit, C., & Rousset, G. 2008, *Proc. SPIE*, 7015, 701573
- Olivier, S. S., & Gavel, D. T. 1994, *J. Opt. Soc. Am. A*, 11, 368
- Racine, R. 2006, *PASP*, 118, 1066
- Sasiela, R. J. 1994, *J. Opt. Soc. Am. A*, 11, 379
- Sarazin, M., & Tokovinin, A. 2002, *ESO Conference and Workshop Proceedings*, 58, 321
- Saunders, W., Gillingham, P., McGrath, A., Haynes, R., Brzeski, J., Storey, J., & Lawrence, J. 2008, *Proc. SPIE*, 7012, 70124F
- Storey, J. W. V., Angel, J. R. P., Ashley, M. C. B., Burton, M. G., Hinz, P. M., & Lawrence, J. S. 2006, *Proc. SPIE*, 6267, 62671E
- Strassmeier, K. G., et al. 2007, *Astron. Nach.*, 328, 451
- Tosti, G., et al. 2006, *Proc. SPIE*, 6267, 62671H
- Travouillon, T., Ashley, M. C. B., Burton, M. G., Storey, J. W. V., & Lowenstein, R. F. 2003, *A&A*, 400, 1163
- Trinquet, H., Agabi, A., Vernin, J., Azouit, M., Aristidi, E., & Fossat, E. 2008, *PASP*, 120, 203
- Walden, V. P., Town, M. S., Halter, B., & Storey, J. W. V. 2005, *PASP*, 117, 300
- Ziad, A., Aristidi, E., Agabi, A., Borgnino, J., Martin, F., & Fossat, E. 2008, *A&A*, in press